MOTION-COMPENSATED IMAGE RECONSTRUCTION WITH ALTERNATING MINIMIZATION

Jang Hwan Cho, Sathish Ramani and Jeffrey A. Fessler

ABSTRACT

Cardiac computed tomography (CT) is important for its use in diagnosing heart disease. Motion artifacts are a significant issue for cardiac CT image reconstruction. Motion-compensated image reconstruction (MCIR) has the potential to overcome the drawbacks of conventional gated reconstruction methods by exploiting all the measurement data and using motion information. However, MCIR methods are computationally expensive: the system matrix has both the forward-projector and the warp matrices that make it hard to precondition or to apply block iterative algorithms such as ordered-subsets (OS). In this study, we propose a novel approach to solve the image reconstruction part of the MCIR method more efficiently. We use a variable-splitting technique to dissociate the original problem into a number of simpler problems. The proposed method is amenable to preconditioning, parallelization, and application of block iterative algorithms to sub-problems. We demonstrated through a phantom simulation that with simple diagonal or circulant preconditioners, the proposed method shows good convergence rate compared to conjugate gradient (CG) method.

1. INTRODUCTION

Even with the fast acquisition speed of commercial scanners, motion artifacts such as blurring and streaks are still a significant issue in CT image reconstruction, especially for cardiac CT imaging. Various methods have been proposed to address this problem [1, 2]. Many of these are gated reconstruction methods that use only the projection data corresponding to approximately the same motion state. Such methods can provide promising results in terms of image quality and processing time. However, they suffer from limitations such as dose inefficiency and limited temporal resolution. Especially for fast and arhythmic cardiac motion, such methods may be subjected to residual motion artifacts [3].

To overcome the limitations of gated reconstruction, a variety of motion-compensated image reconstruction methods (MCIR) have been proposed in the literature [3, 4]. MCIR methods can exploit all collected data and motion information to obtain reconstructed images with better dose efficiency. In general, MCIR methods consist of two main steps: estimating the motion and reconstructing the image using the estimated motion. The quality of the reconstructed image is significantly affected by the accuracy of the estimated motion, and thus many researchers have focussed on improving motion estimates. However, the image reconstruction part is also very important for practical use of MCIR methods. Since the system model in MCIR methods has both the forward-projector and the warp matrices, it becomes computationally very expensive to use iterative algorithms for MCIR. Unlike conventional CT image reconstruction problems, designing a proper preconditioner for MCIR is not trivial due to the complexity of the system model. Ordered-subset (OS) type of algorithms are not efficient for MCIR, especially when when warping is computationally expensive.

In this paper, we propose a novel approach to solve the image reconstruction part of MCIR method more efficiently. We use a variable-splitting technique to dissociate the original problem into a number of simpler problems that are then solved individually.

This work is supported by GE Healthcare.

The authors are with the Electrical Engineering and Computer Science Department, University of Michigan, Ann Arbor, MI 48109-2122 USA

2. MOTION-COMPENSATED IMAGE RECONSTRUCTION FOR CT

2.1. Measurement Model

Let $\boldsymbol{x}(\boldsymbol{r}, t)$ denote the time-dependent attenuation coefficient distribution of the unknown object, where $\boldsymbol{r}$ is the spatial location and t is time. Let t_m be the time of mth frame at which the measurements, $\boldsymbol{y}_m$, corresponding to the motion-free state of the objects are acquired. We assume that the measurements consist of N_f scans, $\boldsymbol{y} = [\boldsymbol{y}_1, \cdots, \boldsymbol{y}_{N_f}]$. The measurements were assumed to be linearly related to the object $\boldsymbol{x}_m = \boldsymbol{x}(\cdot, t_m)$ as follows:

$$\boldsymbol{y}_m = \boldsymbol{A}_m \boldsymbol{x}_m + \epsilon_m, \quad m = 1, \cdots, N_f, \tag{1}$$

where $\boldsymbol{A}_m$ is the system model for mth frame and ϵ_m is the noise. The goal is to reconstruct $\{\boldsymbol{x}_m\}$ from $\{\boldsymbol{y}_m\}$ using a motion model. Here we assume $\boldsymbol{x}_m = \boldsymbol{T}_m \boldsymbol{x}$ where $\boldsymbol{T}_m$ is a warp matrix based on motion estimates that are determined separately.

2.2. Problem Formulation

Consider a penalized-likelihood least squares (PWLS) formulation of motion-compensated CT image reconstruction:

$$\hat{\boldsymbol{x}} = \arg\min_{\boldsymbol{x}} \{\Psi(\boldsymbol{x}) \triangleq \mathsf{Ł}(\boldsymbol{x}) + \mathsf{R}(\boldsymbol{Cx})\}, \tag{2}$$

$$\mathsf{Ł}(\boldsymbol{x}) = \frac{1}{2}\|\boldsymbol{y} - \boldsymbol{ATx}\|^2_{\boldsymbol{W}}, \quad \mathsf{R}(\boldsymbol{Cx}) = \beta \sum_{k=1}^{K} \kappa_k \, \psi_k([\boldsymbol{Cx}]_k),$$
$$\boldsymbol{A} = \mathrm{diag}\{\boldsymbol{A}_1, \cdots, \boldsymbol{A}_{N_f}\}, \quad \boldsymbol{T} = [\boldsymbol{T}_1' \ldots \boldsymbol{T}_{N_f}']',$$

where $\boldsymbol{A}$ is the system matrix, $\boldsymbol{x} \in \mathbb{R}^N$ is the discretized version of the object being reconstructed, $\boldsymbol{W} = \mathrm{diag}\{w_i\}$ is a statistical weighting matrix, β is the regularization parameter, κ_k is the user-defined weight for controlling spatial resolution in the reconstructed image, ψ_k is the potential function, $\boldsymbol{C}$ is a matrix that performs finite differences between neighboring voxels, K is the number of neighbors, and $\boldsymbol{T}$ is the warp matrix. The minimization problem (2) is challenging due to the warp matrix $\boldsymbol{T}$ in the system model.

3. PROPOSED METHOD

We apply a variable splitting approach to the problem. The basic idea of variable splitting method is to introduce auxiliary constraint variables so that coupled parts in the cost function can be separated [5]. The original problem is transformed into an equivalent constrained optimization problem, and then alternating minimization methods are applied to efficiently solve the problem. Previous works have focussed on splitting the regularization term and also the statistical weighting [6]. In this work, in addition to those splittings, we focus on splitting the warp matrix from the forward-projector in the system matrix.

3.1. Equivalent Constrained Optimization Problem

We introduce auxiliary constraint variables $\boldsymbol{u}$, $\boldsymbol{v}$, $\boldsymbol{z}$, and $\boldsymbol{s}$, and write (2) as the following equivalent constrained problem:

$$\arg\min_{\boldsymbol{x},\boldsymbol{u},\boldsymbol{v},\boldsymbol{z},\boldsymbol{s}} \Psi(\boldsymbol{x},\boldsymbol{u},\boldsymbol{v},\boldsymbol{z},\boldsymbol{s}) = \frac{1}{2}\|\boldsymbol{y} - \boldsymbol{v}\|^2_{\boldsymbol{W}} + \mathsf{R}(\boldsymbol{z}),$$

$$s.t. \quad \boldsymbol{u} = \boldsymbol{Tx}, \quad \boldsymbol{v} = \boldsymbol{Au}, \quad \boldsymbol{z} = \boldsymbol{Cs}, \quad \boldsymbol{s} = \boldsymbol{x}, \tag{3}$$

where $\boldsymbol{u} \in \mathbb{R}^{NN_f}$ separates the system matrix from the warp matrix, $\boldsymbol{v} \in \mathbb{R}^M$ separates the effect of the weighting matrix, $\boldsymbol{W}$, on $\boldsymbol{Ax}$, $\boldsymbol{z} \in \mathbb{R}^{NK}$ and $\boldsymbol{s} \in \mathbb{R}^N$ detach the warp matrix from the regularizer.

3.2. Method of Multipliers

We used the framework of method of multipliers [7] to solve (3), and constructed an augmented Lagrangian function as follows:

$$\begin{aligned} L(\boldsymbol{x},\boldsymbol{u},\boldsymbol{v},\boldsymbol{z},\boldsymbol{s}) &\triangleq \frac{1}{2}\|\boldsymbol{y} - \boldsymbol{v}\|^2_{\boldsymbol{W}} + \mathsf{R}(\boldsymbol{z}) \\ &+ \frac{\mu_{\boldsymbol{u}}}{2}\|\boldsymbol{u} - \boldsymbol{Tx} - \eta_{\boldsymbol{u}}\|^2 + \frac{\mu_{\boldsymbol{v}}}{2}\|\boldsymbol{v} - \boldsymbol{Au} - \eta_{\boldsymbol{v}}\|^2 \\ &+ \frac{\mu_{\boldsymbol{z}}}{2}\|\boldsymbol{z} - \boldsymbol{Cs} - \eta_{\boldsymbol{z}}\|^2 + \frac{\mu_{\boldsymbol{s}}}{2}\|\boldsymbol{s} - \boldsymbol{x} - \eta_{\boldsymbol{s}}\|^2, \end{aligned} \tag{4}$$

where η's are Lagrange-multiplier-like vectors and μ's are the AL penalty parameters (see [6] for details).

Solving (3) using the AL function would require jointly minimizing (4) with respect to all variables which is computationally expensive. So we apply to alternating minimization [6].

3.3. Alternating Direction Minimization

At the jth iteration, we update each vector in turn as follows:

$$\begin{aligned}
\boldsymbol{x}^{(j+1)} &= \arg\min_{\boldsymbol{x}} \frac{\mu_{\boldsymbol{u}}}{2}\left\|\boldsymbol{u}^{(j)} - \boldsymbol{Tx} - \eta_{\boldsymbol{u}}^{(j)}\right\|^2 \\
&\quad + \frac{\mu_{\boldsymbol{s}}}{2}\left\|\boldsymbol{s}^{(j)} - \boldsymbol{x} - \eta_{\boldsymbol{s}}^{(j)}\right\|^2, && (5)\\
\boldsymbol{u}^{(j+1)} &= \arg\min_{\boldsymbol{u}} \frac{\mu_{\boldsymbol{u}}}{2}\left\|\boldsymbol{u} - \boldsymbol{Tx}^{(j+1)} - \eta_{\boldsymbol{u}}^{(j)}\right\|^2 \\
&\quad + \frac{\mu_{\boldsymbol{v}}}{2}\left\|\boldsymbol{v}^{(j)} - \boldsymbol{Au} - \eta_{\boldsymbol{v}}^{(j)}\right\|^2, && (6)\\
\boldsymbol{v}^{(j+1)} &= \arg\min_{\boldsymbol{v}} \frac{1}{2}\|\boldsymbol{y} - \boldsymbol{v}\|^2_{\boldsymbol{W}} \\
&\quad + \frac{\mu_{\boldsymbol{v}}}{2}\left\|\boldsymbol{v} - \boldsymbol{Au}^{(j+1)} - \eta_{\boldsymbol{v}}^{(j)}\right\|^2, && (7)\\
\boldsymbol{s}^{(j+1)} &= \arg\min_{\boldsymbol{s}} \frac{\mu_{\boldsymbol{z}}}{2}\left\|\boldsymbol{z}^{(j)} - \boldsymbol{Cs} - \eta_{\boldsymbol{z}}^{(j)}\right\|^2 \\
&\quad + \frac{\mu_{\boldsymbol{s}}}{2}\left\|\boldsymbol{s} - \boldsymbol{x}^{(j+1)} - \eta_{\boldsymbol{s}}^{(j)}\right\|^2, && (8)\\
\boldsymbol{z}^{(j+1)} &= \arg\min_{\boldsymbol{z}} \mathsf{R}(\boldsymbol{z}) \\
&\quad + \frac{\mu_{\boldsymbol{z}}}{2}\left\|\boldsymbol{z} - \boldsymbol{Cs}^{(j+1)} - \eta_{\boldsymbol{z}}^{(j)}\right\|^2, && (9)\\
\eta_{\boldsymbol{u}}^{(j+1)} &= \eta_{\boldsymbol{u}}^{(j)} - (\boldsymbol{u}^{(j+1)} - \boldsymbol{Tx}^{(j+1)}), && (10)\\
\eta_{\boldsymbol{v}}^{(j+1)} &= \eta_{\boldsymbol{v}}^{(j)} - (\boldsymbol{v}^{(j+1)} - \boldsymbol{Au}^{(j+1)}), && (11)\\
\eta_{\boldsymbol{s}}^{(j+1)} &= \eta_{\boldsymbol{s}}^{(j)} - (\boldsymbol{s}^{(j+1)} - \boldsymbol{x}^{(j+1)}), && (12)\\
\eta_{\boldsymbol{z}}^{(j+1)} &= \eta_{\boldsymbol{z}}^{(j)} - (\boldsymbol{z}^{(j+1)} - \boldsymbol{Cs}^{(j+1)}), && (13)
\end{aligned}$$

The sub-problems (5) to (8) are all quadratic problems for which analytical solutions exist. However, (5) and (6) cannot be implemented explicitly due to the enormous sizes of the matrices involved. We employ the iterative CG-solver for these sub-problems.

Sub-problem (5) is an image-registration-type problem, which has the following analytical solution:

$$\boldsymbol{x}^{(j+1)} = \boldsymbol{H}^{-1}(\mu_{\boldsymbol{u}}\boldsymbol{T}'(\boldsymbol{u}^{(j)} - \eta_{\boldsymbol{u}}^{(j)}) + \mu_{\boldsymbol{s}}(\boldsymbol{s}^{(j)} - \eta_{\boldsymbol{s}}^{(j)})), \tag{14}$$

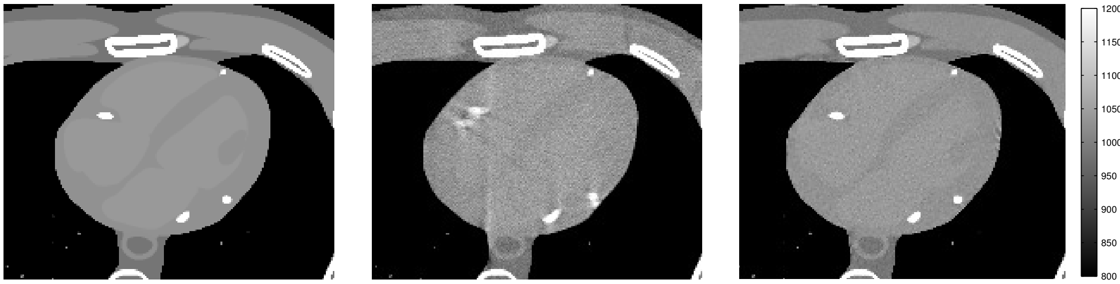

(a) (b) (c)

Fig. 1. Images in the ROI of (a) XCAT phantom, (b) FBP reconstruction with Hanning filter (also the initial guess $\boldsymbol{x}^{(0)}$), (c) Converged Image $\boldsymbol{x}^{(\infty)}$.

where $\boldsymbol{H} = \mu_{\boldsymbol{u}} \boldsymbol{T}'\boldsymbol{T} + \mu_{\boldsymbol{s}} \boldsymbol{I}_N$. We accelerate the CG-solver for (14) by using a suitable preconditioner for $\boldsymbol{H}$. Since $\boldsymbol{H}$ is much simpler than the Hessian of the original data term in (2), it is more amenable to preconditioning.

We now consider (6), which is a tomography problem with the following solution:

$$\boldsymbol{u}^{(j+1)} = \boldsymbol{G}^{-1}(\mu_{\boldsymbol{u}}(\boldsymbol{T}\boldsymbol{x}^{(j+1)} + \eta_{\boldsymbol{u}}^{(j)}) + \mu_{\boldsymbol{v}} \boldsymbol{A}'(\boldsymbol{v}^{(j)} - \eta_{\boldsymbol{v}}^{(j)})),$$

where $\boldsymbol{G} = \mu_{\boldsymbol{v}} \boldsymbol{A}'\boldsymbol{A} + \mu_{\boldsymbol{u}} \boldsymbol{I}_{NN_f}$. We preconditioned this term with a circulant matrix to obtain faster convergence [6, 8]. This sub-problem can be further parallelized into N_f problems. Each parallelized problem can be efficiently solved by preconditioned CG or ordered-subsets type algorithms, which are less efficient for the original problem.

Sub-problems (7) - (9) can be solved much more easily compared to above two sub-problems. Sub-problem (7) has a simple analytical solution, and (8) is exactly solvable with Fourier transform if we use $\boldsymbol{C}$ with periodic end condition. Finally, (9) can be solved easily with iterative algorithms or exactly solved for a variety of potential functions. Here, we consider one of the edge-preserving regularization using the Fair potential function. For this regularizer, (9) separates into 1D minimization problems and has an exact solution (See [6] for details). The AL parameters, μ's, mainly govern the convergence speed of the proposed splitting method [6]; we selected them empirically to achieve good convergence speed.

4. RESULTS

The proposed algorithm was investigated on a 2D CT image reconstruction problem with cardiac motion for simulated data. We simulated a 3rd-generation fan-beam CT system using the separable footprint projector [9]. The simulated system has 888 channels per view spaced 1.0239 mm apart, and 984 evenly spaced view angles over 360°. The image was reconstructed to a 512 $\times$ 512 grid of 0.9766 mm pixels. We generated seven frames of the XCAT phantom for a heart rate of 75 bpm. The motion between the frames was estimated directly from XCAT images using nonrigid image registration.

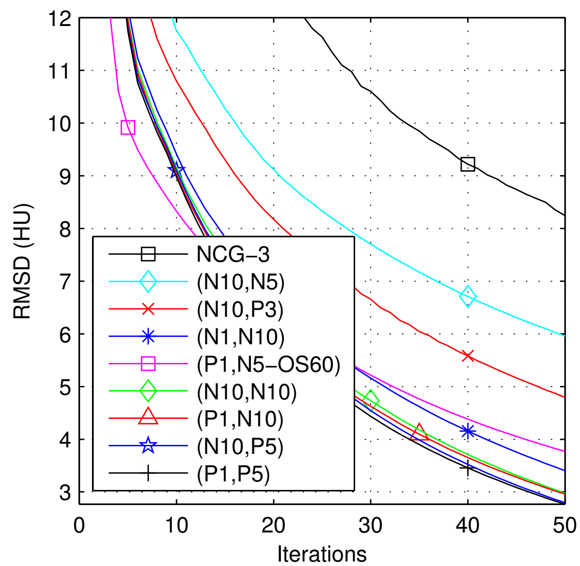

Fig. 2. Plot of RMSD versus iteration for various settings of the proposed method compared to the conventional CG method. For the proposed method, (N10,P5) indicates 10 iterations for sub-problem (5) without preconditioner for $\boldsymbol{H}$ and 5 iterations for sub-problem (6) with a preconditioner for $\boldsymbol{G}$. OS60 indicates that ordered subsets method with 60 subsets was used instead of CG.

Estimating motion parameters from true images is unrealistic, but our focus is not on obtaining reasonable motion estimates. We only focus on the image reconstruction part of MCIR. For the regularizer, we used a Fair potential function to provide edge-preservation and a certainty-based penalty to obtain more uniform resolution. The sinogram was generated with Poisson noise, and the weights in the data-fit term in (2) were chosen as $w_i = \exp(-[\boldsymbol{A}\boldsymbol{x}]_i)$. We selected the regularization parameter β such that the target PSF has a full-width at half-maximum (FWHM) of approximately 1.3 mm.

For comparison, we used the (nonlinear) conjugate gradient algorithm to solve the original problem (2). To analyze the convergence speed of the proposed method we computed the root mean squared (RMS) difference between the image estimate at the nth iteration, $\boldsymbol{x}^{(n)}$, with the "fully" converged solution, $\boldsymbol{x}^{\infty}$. For the Fair potential, the original MCIR problem is strictly convex and thus has a unique minimizer, $\boldsymbol{x}^{\infty}$. We numerically approximated $\boldsymbol{x}^{\infty}$ as the mean of the images reconstructed (assuming convergence) by running 1000 iterations of CG and 700 iterations of the proposed method with (10,10) sub-iterations.

Fig. 1 illustrates that the conventional filtered backprojection (FBP) method gives a reconstructed image with severe motion artifacts but the motion-compensated image, on the contrary, contains much less motion artifacts. Some residual motion artifacts still exist due to imperfect motion estimates even though they were obtained directly from the true XCAT images.

Fig. 2 illustrates that the proposed method converges much faster in iterations compared to the conventional CG method when we use enough sub-iterations with obvious computation overhead. This result suggests that if we have a proper preconditioner for each sub-problem, we can still obtain fast convergence. We also investigated different options for the proposed method summarized in Fig. 2. Using a preconditioner for sub-problems helped reduce the number of sub-iterations while achieving fast convergence speed.

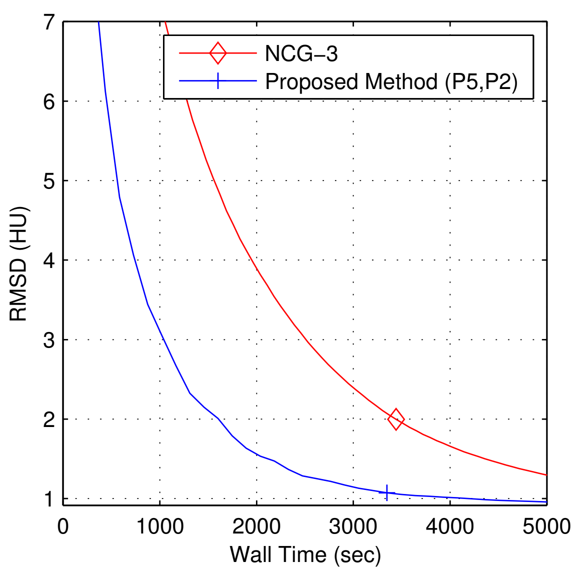

Fig. 3. Plot of RMSD versus wall time for the proposed method compared to the conventional CG method with 3 line-search iterations. A diagonal preconditioner and a circulant preconditioner were used for sub-problems (5) and (6) respectively.

In Fig. 3, we provided the proposed method with sub-optimal preconditioners. We used a simple diagonal preconditioner for (5) based on the diagonal elements of $\boldsymbol{H}$ and a circulant preconditioner for (6) using the fact that $\boldsymbol{G}$ contains $\boldsymbol{A}_m' \boldsymbol{A}_m$, which is approximately shift invariant [6]. The proposed method shows faster convergence speed compared to CG method. While the proposed method as implemented in MATLAB provides marginal improvement in convergence speed over CG, we believe its ability to parallelize some of the update steps can further improve its efficiency.

5. DISCUSSION

We applied a variable splitting approach to the motion-compensated image reconstruction problem. The proposed method has faster convergence speed to conjugate gradient method, and offers the potential for parallelizabilty and preconditioning of sub-problems. Some of the sub-problems can be solved simultaneously or further divided into smaller problems. By using more sophisticated preconditioners for the sub-problems, the performance of the proposed method can be further improved. In this study, we focussed on the image reconstruction part of MCIR, but our method also can be extended to the joint estimation framework. Our future work will focus on improving the convergence speed of the proposed method and on applying it to 3-D CT.

6. REFERENCES

[1] M. Grass, R. Manzke, T. Nielsen, P. Koken, R. Proksa, M. Natanzon, and G. Shechter, "Helical cardiac cone beam reconstruction using retrospective ECG gating," *Phys. Med. Biol.*, vol. 48, no. 18, pp. 3069–84, Sep. 2003.

[2] E. Hansis, D. Schäfer, O. Dössel, and M. Grass, "Projection-based motion compensation for gated coronary artery reconstruction from rotational x-ray angiograms," *Phys. Med. Biol.*, vol. 53, no. 14, pp. 3807–20, Jul. 2008.

[3] A. A. Isola, A. Ziegler, T. Koehler, W. J. Niessen, and M. Grass, "Motion-compensated iterative cone-beam CT image reconstruction with adapted blobs as basis functions," *Phys. Med. Biol.*, vol. 53, no. 23, pp. 6777–98, Dec. 2008.

[4] Q. Tang, J. Cammin, and K. Taguchi, "A fully four-dimensional, iterative motion estimation and compensation for cardiac x-ray computed tomography," in *Proc. Intl. Mtg. on Fully 3D Image Recon. in Rad. and Nuc. Med*, 2011, pp. 470–3.

[5] T. Goldstein and S. Osher, "The split Bregman method for L1-regularized problems," *SIAM J. Imaging Sci.*, vol. 2, no. 2, pp. 323–43, 2009.

[6] S. Ramani and J. A. Fessler, "A splitting-based iterative algorithm for accelerated statistical X-ray CT reconstruction," *IEEE Trans. Med. Imag.*, vol. 31, no. 3, pp. 677–88, Mar. 2012.

[7] J. Nocedal and S. J. Wright, *Numerical optimization*. New York: Springer, 1999.

[8] N. H. Clinthorne, T. S. Pan, P. C. Chiao, W. L. Rogers, and J. A. Stamos, "Preconditioning methods for improved convergence rates in iterative reconstructions," *IEEE Trans. Med. Imag.*, vol. 12, no. 1, pp. 78–83, Mar. 1993.

[9] Y. Long, J. A. Fessler, and J. M. Balter, "3D forward and back-projection for X-ray CT using separable footprints," *IEEE Trans. Med. Imag.*, vol. 29, no. 11, pp. 1839–50, Nov. 2010.